



Published in final edited form as:

Chembiochem. 2007 December 17; 8(18): 2233–2239. doi:10.1002/cbic.200700317.

## Synthesis, Modeling, and Biological Evaluation of Analogues of the Semisynthetic Brevetoxin Antagonist $\beta$ -Naphthoyl-Brevetoxin

Sophie Michelliza<sup>[a]</sup>, William M. Abraham<sup>[b]</sup>, Henry M. Jacocks<sup>[a]</sup>, Thomas Schuster<sup>[a]</sup>, and Daniel G. Baden<sup>[a]</sup>

[a]Dr. S. Michelliza, Dr. H. M. Jacocks, Dr. T. Schuster, Dr. D. G. Baden Center for Marine Science, University of North Carolina Wilmington 5600 Marvin. K. Moss Lane, Wilmington, NC 28409 (USA) Fax: (+1) 910-962-2410 E-mail: michellizas@uncw.edu

[b]Dr. W. M. Abraham Division of Pulmonary and Critical Care Medicine Mount Sinai Medical Center 4300 Alton Road, Miami Beach, FL 33140 (USA)

### Abstract

Brevetoxins are neurotoxic compounds produced by the dinoflagellate *Karenia brevis*. Extensive blooms induce neurotoxic shellfish poisoning (NSP) and asthma-like symptoms in humans.  $\beta$ -naphthoyl-brevetoxin, the first semisynthetic brevetoxin antagonist, has been defined as the lead compound in the investigation of the mechanisms of bronchoconstriction induced by inhaled brevetoxins and relaxation or reversal of those effects by selected derivatives. In pursuit of more potent and effective brevetoxin antagonists, a series of  $\beta$ -naphthoyl-brevetoxin analogues have been synthesized. Activities were determined by competitive displacement of tritiated brevetoxin-3 from rat brain synaptosomes and by lung resistance measurements in sheep. Additionally, preliminary computational structural studies have been performed. All analogues bound to rat brain synaptosomes with affinities similar to  $\beta$ -naphthoyl-brevetoxin but exhibited very different responses in sheep. The biological evaluations along with computational studies suggest that the brevetoxin binding site in rat brain synaptosome might be different from the ones in lung tissue and both steric and electrostatic factors contribute to the efficacy of brevetoxin antagonism.

### Keywords

binding assays; natural products; neurotoxins; polyethers; syntheses

### Introduction

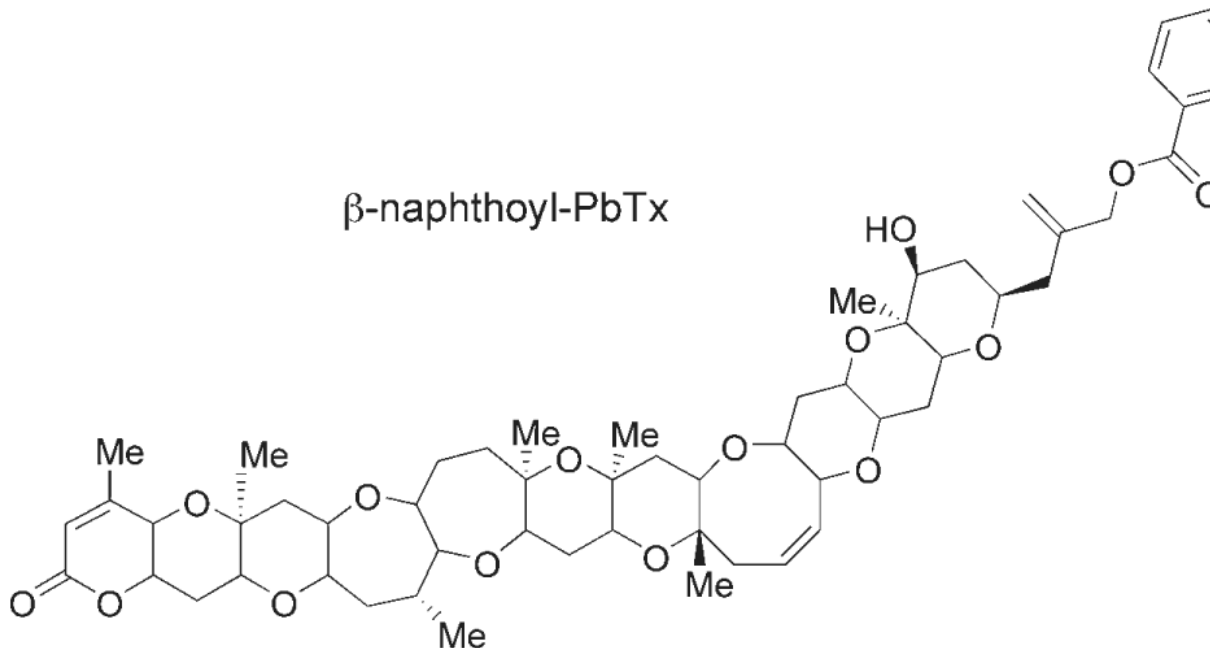
“Red tide” is the name given to an unpredictable phenomenon characterized by ocean blooms of unicellular algae. Brevetoxins[1] (PbTx, Scheme 1) are polyether neurotoxins produced by the marine dinoflagellate *Karenia brevis*, an organism associated with red tide catastrophes that periodically occur along the eastern Atlantic coast and the Gulf of Mexico. Blooms of *K. brevis* cause massive fish kills and adverse health effects in humans and marine mammals. [2] Exposure to brevetoxins generally occurs either by ingestion or through inhalation of aerosolized toxins. Consumption of shellfish contaminated with toxin results in neurotoxic shellfish poisoning (NSP)[3] while brevetoxin inhalation results in upper (nasopharyngeal) and/or lower (bronchial) airway irritation, which if severe enough can result in asthma-like symptoms in susceptible humans.[4]

Brevetoxins are classified into two groups according to their ring system: decacyclic brevetoxin A and undecacyclic brevetoxin B. All toxins exhibit common features[5] including 1) an A-ring “head” electrophilic lactone; 2) a rigid spacer region (five or six rings); 3) a four-ring binding region; and 4) a flexible “tail” region. Brevetoxin-2 (PbTx-2), the most prominent member of the brevetoxin B family, consists of 11 *trans*-fused ether rings condensed in a ladder shape (cylinder, ~ 30 (long) x 6 Å (diameter)), 23 stereogenic centers, and three C=C double bonds (Scheme 1).

Brevetoxins exert their biological activity by binding with high affinity ( $K_d = 1.6 \text{ nM}$ ,  $B_{\text{max}} = 1.9 \text{ pmol per mg protein}$ ) to the  $\alpha$  subunit of voltage-sensitive sodium channels (VSSC)[6] causing activation of the channels and prolonged membrane depolarization.[7] The toxin is believed to orient itself across the membrane, parallel to the  $\alpha$  helices, with the lactone A-ring inward towards the cytoplasm and the K-ring side chain (end of the molecule) pointed outwards towards the extracellular milieu[5a,8] (Figure 1). In the airways, brevetoxins are extremely potent agents. Nanomolar to picomolar concentrations of aerosolized toxins caused bronchoconstriction in sheep.[9]

$\beta$ -Naphthoyl-brevetoxin ( $\beta$ -naphthoyl-PbTx), a synthetic ester analogue of brevetoxin B, has recently been isolated and characterized as the first competitive antagonist to brevetoxin B. [10] This analogue binds with high affinity ( $K_i = 1.2 \text{ nM}$ ) to the VSSC without activating the channel, and competitively displaces brevetoxin in synaptosomal receptor-binding assays in rat sensory neurons. Furthermore,  $\beta$ -naphthoyl-PbTx was shown to block the brevetoxin-induced bronchoconstriction in sheep in a dose-dependent manner with potency consistent with the observed  $K_i$ . [9]

The competitive inhibition by  $\beta$ -naphthoyl-PbTx in synaptosomal binding assays combined with the dose-dependent



inhibitory activity against PbTx in the sheep airways prompted us to initiate a structure—activity relationship study to increase our understanding of the mechanism of  $\beta$ -naphthoyl-PbTx action with the hope of enhancing its affinity/efficacy in the two test systems described

above. Here, we report the synthesis of eight new  $\beta$ -naphthoyl-PbTx analogues, their binding affinities in rat brain synaptosomes and their bronchoconstrictor effects in sheep. Additionally, we carried out preliminary computational studies with  $\beta$ -naphthoyl-PbTx and a selected analogue.

## Results and Discussion

### Chemistry

PbTx-2 and PbTx-3 are extracted from laboratory cultures of *K. brevis* and isolated using a combination of liquid–liquid extraction, combi-flash™ chromatography, fractional crystallization, and HPLC.

As shown in Scheme 2, the common procedure to yield the ester analogues of  $\beta$ -naphthoyl-PbTx involved the treatment of PbTx-3 with the corresponding carboxylic acid in presence of *N,N'*-dicyclohexylcarbodiimide (DCC) and dimethyl aminopyridine (DMAP).

Treatment with a saturated solution of ammonium chloride followed by extraction with ethyl acetate and reverse-phase HPLC purification furnished the diphenyl acetic acid-PbTx-ester (**1**), naphthalene-1-carboxylic acid-PbTx-ester (**2**), naphthalene-2-yl acetic acid-PbTx-ester (**3**), (naphthalene-2-yloxy)acetic acid-PbTx-ester (**4**), 6-fluoro-naphthalen-2-carboxylic acid-PbTx-ester (**5**), and quinoline-3-carboxylic acid-PbTx-ester (**6**) in, respectively, 62, 55, 67, 59, 70, and 55% yield.

Oxidation of PbTx-2 in the presence of sodium chlorite, sodium phosphate, and 2-methylbut-2-ene in *tert*-butanol yielded the PbTx carboxylic acid (**7**) that was then allowed to react with 2-naphthol under the same conditions as previously described to give PbTx acid naphthalene-2-yl ester (“reverse  $\beta$ -naphthoyl-PbTx”, **8**) in 55% yield after purification (Scheme 3)

The ether analogue (**9**, Scheme 4) was synthesized with 65% yield by treatment of PbTx-3 with sodium hydride in the presence of sodium iodide followed by addition of 2-(bromomethyl) naphthalene.

### Biological evaluation

All new  $\beta$ -naphthoyl-PbTx analogues were tested for their binding affinity at site 5 of VSSC by using competitive displacement of tritiated PbTx-3 from rat brain synaptosomes[6a] and for their bronchoconstrictor effect in sheep airways by using lung resistance measurements.[11–13] Inhibition curves showing the displacement of tritiated PbTx-3 by competitor ligands and bronchoconstrictor effects calculated as the percentage increase in lung resistance (RL) from baseline are displayed in Figure 2. Table 1 summarizes equilibrium dissociation constants ( $K_i$ ) values and the RL percentage increases from the baseline values.

Binding of all known naturally occurring PbTxs to VSSC results in sodium channel opening leading to a dose-dependent depolarization of excitable membranes. The putative mechanism includes a conformational change in the VSSC induced by binding of a region of the toxin backbone as site 5 as well as inhibition of channel inactivation by interaction with the A-ring lactone, resulting in a persistent open configuration. Modification of the K-ring side chain has been shown to have, typically, only minor effects on binding, suggesting that the side chain is not directly involved in recognition and binding at site 5. This observation is supported by analysis of the binding data in Figure 2A and Table 1. Introduction of the bulky  $\beta$ -naphthoyl group onto the distal end of the side chain yields a molecule that binds with the same affinity as the parent molecule. Indeed, with the exception of analogue **9**, all derivatives, including the biphenyl analogue **1**, bind to rat brain VSSC with affinities similar to the synthetic antagonist  $\beta$ -naphthoyl-PbTx itself. The  $K_i$  values are in the range of 0.5 to 4.6 nM for analogues **1** through

**8** and 180 nM for the ether analogue **9**; this suggests that the ester carbonyl moiety, with or without conjugation to the naphthalene ring system, is required for maximum synaptosome binding affinity. This also suggests that the ester carbonyl group enhances the stability of the ligand-receptor complex, perhaps by acting as a hydrogen-bond acceptor.

$\beta$ -Naphthoyl-PbTx acts as a channel blocker at neuronal VSSC (i.e. it competitively antagonizes the effects of brevetoxin, but occupation of the binding site by  $\beta$ -naphthoyl-PbTx itself results in no discernible increase in sodium flux).[10] Analysis of the lung resistance measurement data (Figure 2B and Table 1) shows that  $\beta$ -naphthoyl-PbTx causes no bronchoconstriction. If toxin effects at pulmonary sites are analogous to effects in neuronal VSSC, binding of  $\beta$ -naphthoyl-PbTx results in an open channel configuration because the toxin backbone (putative binding region) has not changed. Since there is no increased sodium flux, this implies that the channel pore has been blocked by the  $\beta$ -naphthoyl moiety. Although  $\beta$ -naphthoyl-PbTx itself causes no bronchoconstriction, all the new  $\beta$ -naphthoyl-PbTx analogues induced moderate to significant bronchoconstrictor effects with an increase over baseline values from 34 to 88%. To extend the neuronal analogy further, it is reasonable to hypothesize that increases in bronchoconstriction seen in the presence of brevetoxins and analogues is due to increased sodium flux into target pulmonary cells. This suggests that the more completely the compound blocks the channel, the lower the RL value.

The RL measurements of **3** and **4** have revealed that introduction of a spacer region between the ester carbonyl moiety and the naphthalene moiety resulted in a moderate constrictor effect, whereas these two analogues bind with affinities similar to  $\beta$ -naphthoyl-PbTx in rat brain synaptosomes. It appears that the inhibition of the PbTx-induced bronchoconstriction is related to the length of the side chain. Changing the naphthalene moiety into a quinoline moiety resulted in a significant bronchoconstrictor effect in sheep which can be explained by the introduction of an extra electron-pair donor in the quinoline moiety.

Interestingly, compound **2** which differs from  $\beta$ -naphthoyl-PbTx by one position on the naphthalene ring resulted in a 34% increase in lung resistance. The change in position of the bond between PbTx and the naphthalene ring system (see compound **2**) might have introduced a more constraining and planar shape than that of  $\beta$ -naphthoyl-PbTx providing less freedom of rotation around the bond, therefore leaving the pore partially unobstructed and allowing the sodium ion flux. Compound **5**, which possesses an electron-withdrawing group showed an even greater constrictor effect (62%). Bronchoconstriction effects have also been induced by just reversing the ester linkage (see analogue **8**). In the  $\beta$ -naphthoyl-PbTx derivative, the naphthalene moiety is conjugated with the ester carbonyl whereas in the “reverse  $\beta$ -naphthoyl-PbTx” **8**, this conjugation is absent. This difference of electronic effects might explain the bronchoconstrictor response induced by **8** relative to  $\beta$ -naphthoyl-PbTx. Finally, RL measurements of **6** and **9** exhibited the same significant constrictor response whereas **9** binds 100 times less avidly than **6**.

In summary, the binding and bronchoconstriction results suggest that: 1) the brevetoxin binding site in rat brain synaptosomes might be different from the brevetoxin binding site in lung tissues; 2) binding affinity does not quantitatively translate into bronchoconstrictor response; or 3) the sodium channel function is differentially modulated by the substituent group of  $\beta$ -naphthoyl-PbTx or analogues, respectively. As discussed above, the data also suggest that both steric and electrostatic factors contribute to the efficacy of the blockade.

### Computational methods

In an attempt to explain the extraordinary pharmacological behavior of  $\beta$ -naphthoyl-PbTx and its analogues, preliminary computational studies were carried out on  $\beta$ -naphthoyl-PbTx and the “reverse  $\beta$ -naphthoyl-PbTx” **8**. Searches with the Metropolis Criterion, both random walk

and usage-directed, revealed that both compounds have a strong preference for a ground state with the residue folded over the ring backbone (Figure 3A). It has been speculated that the conformational preferences are due to the optimization of lipophilic and electronic interactions between the naphthyl groups and the polyketide backbone. Computational searches for unfolded conformers found one unfolded stable conformer for the “reverse  $\beta$ -naphthoyl-PbTx” analogue **8**, which is 5.5 kcal mol<sup>-1</sup> higher in energy than the folded form, while the stable exocyclic rotamer for the  $\beta$ -naphthoyl-PbTx derivative is 17.0 kcal mol<sup>-1</sup> higher in energy than its folded form. This suggests that for the “reverse  $\beta$ -naphthoyl-PbTx” analogue both the folded and the open forms, are available at ambient temperature. To contrast this, the  $\beta$ -naphthoyl derivative is essentially locked in a folded position under the assumption of a Boltzmann distribution for the different states. The geometric restraints for the “reverse  $\beta$ -naphthoyl-PbTx” analogue and  $\beta$ -naphthoyl-PbTx derivatives differ. Since the “reverse  $\beta$ -naphthoyl-PbTx” analogue contains a metacrylate-type functionality, the side chain is bonding-angle and conjugatively constrained and cannot fully extend across the brevetoxin backbone (Figure 3B), restricting it to a coplanar parallel arrangement with the backbone only. In comparison, the  $\beta$ -naphthoyl substituent extends antiparallel across the polyketide backbone, as the position of the naphthyl functionality is fixed through the conjugation between the carbonyl group and the naphthyl ring, while the side chain has more conformational freedom. Figure 3A and B show the naphthyl-groups on the *alpha* side of the molecule, which is favored in the current calculations by a small energy difference relative to positioning the residue on the *beta* face. Detailed computational studies with the remaining  $\beta$ -naphthoyl-PbTx analogues mentioned above are in progress and will be described in future publications.

## Conclusions

Although the new analogues of  $\beta$ -naphthoyl-PbTx did not show enhanced antagonist activity, the dichotomy between the synaptosomal binding data and the pulmonary consequences suggests the possibility of different binding sites in the two tissues. It is clear that there is a profound difference in the bronchoconstrictor potential between natural PbTx-2 (RL = 226  $\pm$  21%) and the complete antagonist  $\beta$ -naphthoyl-PbTx (RL = 0). We believe that side-chain derivatives of the brevetoxins reported herein will further our understanding of how inhaled brevetoxins induce bronchoconstriction and how selected derivatives relax or reverse those effects. This data might reveal important information about the mechanisms of inhalation toxicity by these potent aerosols. Further experiments are in progress to characterize the brevetoxin binding site in lung tissues and to further elucidate the unique features that make  $\beta$ -naphthoyl-PbTx the only “pure” antagonist-against brevetoxin in this series.

## Experimental Section

### Synaptosome binding assay

A competitive displacement of tritiated PbTx-3 bound to rat brain synaptosomes was performed on each analogue. Total binding was measured using the previously described centrifugation technique.[7a] Synaptosomes were prepared by the method of Dodd et al.[14] from whole rat brain (male, Sprague-Dawley). All preparations and media contained a protease inhibitor cocktail. For measurements of equilibrium dissociation constants ( $K_i$ ), competitor concentration ranged from 0 to 10  $\mu$ M and the concentration of [<sup>3</sup>H]-PbTx-3 was held constant (approximately 1.5 nM). Nonlinear regression analysis was performed by using GraphPad Prism (v. 4.0). All derived values are the mean of at least three experiments, with duplicate or triplicate determination at each concentration of inhibitor in each experiment. Inhibition curves showing the displacement of tritiated PbTx-3 by competitor ligands are shown in Figure 2. The  $K_i$  values (the inhibitor concentration necessary to displace half of the radiolabeled toxin specifically bound to the synaptosomes) are summarized in Table 1.

## Lung resistance measurement

A balloon catheter is advanced through one nostril into the lower esophagus, and the animals are intubated with a cuffed endotracheal tube through the other nostril. Pleural pressure is measured through an esophageal catheter. Lateral pressure in the trachea is measured with a side-hole catheter advanced through and positioned distal to the tip of the endotracheal tube. Transpulmonary pressure, the difference between tracheal and pleural pressure, is measured with a differential pressure transducer. To measure RL, the proximal end of the endotracheal tube is connected to a pneumotrachograph, and the signals representing flow and transpulmonary pressure are recorded by computer. Respiratory volume is obtained by digital integration of the flow signal so that RL is calculated from transpulmonary pressure and flow at isovolumetric points. Analysis of 5-10 breaths is used for each determination of RL.  $\beta$ -naphthoyl-brevetoxin analogues were delivered into the airways as aerosols.

The Animal Research Laboratory at Mount Sinai Medical Center is accredited by the American Veterinary Association for Accreditation of Laboratory Animal Care and has filed an assurance statement with the NIH (A-3044-01). The animal research facility adheres to all requirements and provisions of the Animal Welfare Act, PHS policies on animal care and use, and USDA regulations. All animal protocols have been reviewed and approved and are overseen by a consultant veterinarian and an institutional veterinarian.

## Computational calculations

Computations were performed with HyperChem 7.51 (Hypercube Inc., Cambridge, Massachusetts) on Windows XP Professional SP2. The molecular-mechanics force field employed was MM + (Polak-Ribiere convergence algorithm). Metropolis Criterion conformational searches were conducted in vacuo. Molecular dynamics for end-point testing was performed using conventional in vacuo settings without constant temperature considerations. Model-build and search criteria were unrestricted with the exception of the inversion of stereo-centers. The stereo-chemistry for the calculations was chosen based on the relative stereochemistry conventionally described by X-ray crystallography.

## Structure elucidation and synthesis

$^1\text{H}$  and  $^{13}\text{C}$  NMR spectra were recorded in  $[\text{D}_6]$ acetone (99.9 atom% D) on a Bruker Avance 500 MHz NMR. Chemical shifts are reported as  $\delta$  values (ppm) relative to an internal standard of acetone. High-resolution mass spectra were obtained from the mass spectroscopy facility at the Center for Marine Science, UNC Wilmington on an Applied Biosystems QStar XL mass spectrometer in positive-ion mode by direct injection through an Agilent 1100 HPLC system, equipped with a binary pump and an autosampler. The solvent system for infusion consisted of 98% acetonitrile, 2% water, and 0.01% formic acid. Sample concentrations were approximately  $0.01 \text{ mg mL}^{-1}$ , and  $3 \mu\text{L}$  of sample were injected. The instrument was mass-calibrated relative to a mixture of poly(propylene glycol) reference standard before each sample. The acquisition software was Analyst QS 1.1. All reagents were commercial quality and used without further purification. All solvents used were HPLC grade and distilled before use if needed. Starting materials (PbTx-2 and PbTx-3), intermediates, and final products were purified by reverse phase HPLC (90% methanol followed by 100% methanol) using a Varian Dynamax  $250 \times 10.0 \text{ mm}$  Microsorb 100-5  $\text{C}_{18}$  and monitored by UV at 215 nm.

**Procedure A: Preparation of naphthalene-carboxylic acid PbTx esters (1–5) and quinoline carboxylic acid PbTx ester 6**—To a solution of the corresponding carboxylic acids ( $22.88 \mu\text{mol}$ ) in anhydrous  $\text{CH}_2\text{Cl}_2$  (4 mL) DCC (5.06 mg,  $24.55 \mu\text{mol}$ ), PbTx-3 (10 mg,  $11.16 \mu\text{mol}$ ) and DMAP (0.14 mg,  $1.12 \mu\text{mol}$ ) were added. The mixture was allowed to stir at room temperature overnight and then quenched with a saturated solution of ammonium chloride. The aqueous layer was extracted with ethyl acetate ( $4 \times 10 \text{ mL}$ ). The organic layers

were combined, washed with water (10 mL) and brine (10 mL), dried over Na<sub>2</sub>SO<sub>4</sub>, filtered and concentrated under pressure. The crude extracts were purified by HPLC (90% methanol followed by 100% methanol) to yield diphenyl acetic acid-PbTx-ester (**1**), naphthalene-1-carboxylic acid-PbTx-ester (**2**), naphthalene-2-yl acetic acid-PbTx-ester (**3**), (naphthalene-2-yloxy)acetic acid-PbTx-ester (**4**), 6-fluoro-naphthalen-2-carboxylic acid-PbTx-ester (**5**), and quinoline-3-carboxylic acid-PbTx-ester (**6**) in respectively 62, 55, 67, 59, 70, and 55% yield.

#### Diphenyl acetic acid-PbTx-ester (**1**)

<sup>1</sup>H NMR ([D<sub>6</sub>]acetone): δ = 7.38 (m, 4 H), 7.35 (m, 4 H), 7.25 (m, 2 H), 5.76 (dd, *J* = 5.5, 11 Hz, 1 H), 5.68 (m, 2 H), 5.18 (s, 1 H), 4.99 (m, 1 H), 4.95 (m, 1 H), 4.67 (q, 2H, *J* = 13.3 Hz), 4.39 ppm (m, 1 H); <sup>13</sup>C NMR ([D<sub>6</sub>]acetone): δ = 163.66, 161.85, 143.67, 140.16, 136.85, 129.58, 129.40, 128.03, 127.44, 116.26, 114.90 ppm; HRMS (ESI): calcd for C<sub>64</sub>H<sub>83</sub>O<sub>15</sub>: 1091.5740 [*M*+H]<sup>+</sup>; found: 1091.5732.

#### Naphthalene-1-carboxylic acid-PbTx-ester (**2**)

<sup>1</sup>H NMR ([D<sub>6</sub>]acetone): δ = 8.94 (d, *J* = 8.8 Hz, 1 H), 8.29 (dd, *J* = 1.4, 7.3 Hz, 1 H), 8.18 (d, *J* = 8.2 Hz, 1 H), 8.02 (d, *J* = 7.7 Hz, 1 H), 7.65 (m, 4 H), 5.72 (dd, *J* = 5.2, 10.6 Hz, 1 H), 5.68 (m, 2 H), 5.25 (d, *J* = 1.55 Hz, 1 H), 5.11 (s, 1 H), 4.94 ppm (q, *J* = 12.5 Hz, 2 H); <sup>13</sup>C NMR ([D<sub>6</sub>]acetone): δ = 167.47, 163.66, 161.84, 144.11, 136.82, 134.99, 134.36, 132.23, 132.07, 131.14, 129.63, 128.02, 127.39, 127.31, 126.54, 125.76, 116.27, 115.05 ppm; HRMS (ESI): calcd for C<sub>61</sub>H<sub>79</sub>O<sub>15</sub>: 1051.5419 [*M*+H]<sup>+</sup>; found: 1051.5474.

#### Naphthalene-2-yl acetic acid-PbTx-ester (**3**)

<sup>1</sup>H NMR ([D<sub>6</sub>]acetone): δ = 7.87 (m, 2 H), 7.82 (s, 1 H), 7.49 (m, 2 H), 5.76 (dd, *J* = 5.6, 11.4 Hz, 1 H), 5.68 (m, 2 H), 5.03 (d, *J* = 1.3 Hz, 1 H), 4.95 (s, 1 H), 4.61 (q, *J* = 13.4 Hz, 2 H), 4.39 ppm (m, 1 H); <sup>13</sup>C NMR ([D<sub>6</sub>]acetone): δ = 171.97, 164.15, 162.33, 144.26, 137.34, 135.01, 133.96, 133.74, 129.38, 129.15, 126.02, 127.95, 127.57, 127.18, 116.76, 115.10 ppm; HRMS (ESI): calcd for C<sub>62</sub>H<sub>81</sub>O<sub>15</sub>: 1065.5575 [*M*+H]<sup>+</sup>; found: 1065.5555.

#### (Naphthalene-2-yloxy)acetic acid-PbTx-ester (**4**)

<sup>1</sup>H NMR ([D<sub>6</sub>]acetone): δ = 7.83 (m, 2 H), 7.79 (m, 1 H), 7.44 (m, 1 H), 7.36 (m, 1 H), 7.29 (m, 1 H), 7.23 (m, 1 H), 5.75 (dd, *J* = 5.5, 11 Hz, 1 H), 5.67 (m, 2 H), 5.11 (m, 1 H), 5.05 (m, 1 H), 4.92 (s, 2 H), 4.71 ppm (q, *J* = 13.4 Hz, 2 H); <sup>13</sup>C NMR ([D<sub>6</sub>]acetone): δ = 169.70, 164.19, 162.37, 157.58, 143.99, 137.39, 136.10, 131.04, 129.42, 129.09, 128.37, 128.00, 125.39, 119.98, 116.84, 115.69, 108.65 ppm; HRMS (ESI): calcd for C<sub>62</sub>H<sub>81</sub>O<sub>16</sub>: 1081.5525 [*M*+H]<sup>+</sup>; found: 1081.5558.

#### 6-Fluoronaphthalen-2-carboxylic acid-PbTx-ester (**5**)

<sup>1</sup>H NMR ([D<sub>6</sub>]acetone): δ = 8.73 (s, 1 H), 8.23 (dd, *J* = 5.7, 9.2 Hz, 1 H), 8.13 (dd, *J* = 1.4, 8.5 Hz, 1 H), 8.04 (d, *J* = 8.7 Hz, 1 H), 7.74 (dd, *J* = 2.7, 10.0 Hz, 1 H), 7.49 (dt, *J* = 2.6, 8.9 Hz, 1 H), 5.66 (m, 3 H), 5.23 (d, *J* = 1.6 Hz, 1 H), 5.09 (s, 1 H), 4.93 ppm (q, *J* = 1.1 Hz, 2 H); <sup>13</sup>C NMR ([D<sub>6</sub>]acetone): δ = 166.41, 163.64, 161.82, 144.24, 136.74, 133.48, 133.41, 131.76, 130.75, 128.82, 128.77, 127.38, 127.17, 118.28, 118.07, 116.32, 114.94, 112.01, 111.84 ppm; HRMS (ESI): calcd for C<sub>61</sub>H<sub>78</sub>FO<sub>15</sub>: 1069.5325 [*M*+H]<sup>+</sup>; found: 1069.5335.

#### Quinoline-3-carboxylic acid-PbTx-ester (**6**)

<sup>1</sup>H NMR ([D<sub>6</sub>]acetone): δ = 9.41 (d, *J* = 2.1 Hz, 1 H), 9.01 (d, *J* = 2.0 Hz, 1 H), 8.17 (m, 2 H), 7.94 (m, 1 H), 7.74 (m, 1 H), 5.68 (m, 3 H), 5.26 (m, 1 H), 5.12 (m, 1 H), 4.94 ppm (m, 2 H); <sup>13</sup>C NMR ([D<sub>6</sub>]acetone): δ = 149.74, 138.54, 135.89, 132.10, 129.60, 129.44, 127.72,

126.57, 115.43, 114.38 ppm; HRMS (ESI): calcd for  $C_{60}H_{78}NO_{15}$ : 1052.5371 [ $M+H$ ]<sup>+</sup>; found: 1052.5425.

**Procedure B: Preparation of PbTx acid naphthalene-2-yl ester (8)**—2-methylbut-2-ene (70  $\mu$ L, 140  $\mu$ mol),  $Na_2HPO_4$  (4.63 mg, 33.5  $\mu$ mol), and sodium chlorite (6.32 mg, 70  $\mu$ mol) were added at room temperature to a solution of PbTx-2 (10 mg, 11.12  $\mu$ mol) in *t*BuOH (5 mL) and stirred at room temperature for 4 h. The reaction mixture was then quenched with a saturated solution of oxalic acid, and the aqueous layer was extracted with  $Et_2O$  (4  $\times$  10 mL). The organic layers were combined, washed with brine, dried over  $Na_2SO_4$ , filtered, and the solvent was evaporated under pressure. The crude extract was purified by HPLC (90% isocratic methanol) to give compound **7** (8.68 mg, 85% yield). To a solution of the carboxylic acid **7** (10.99  $\mu$ mol) in anhydrous  $CH_2Cl_2$  (4 mL) DCC (5 mg, 24.17  $\mu$ mol) was added, followed by 2-naphthol (2.57 mg, 22.52  $\mu$ mol) and DMAP (0.14 mg, 1.12  $\mu$ mol). The mixture was allowed to stir at room temperature overnight and then quenched with a saturated solution of ammonium chloride. The aqueous layer was extracted with ethyl acetate (4  $\times$  10 mL). The organic layers were combined, washed with water (10 mL) and brine (10 mL), dried over  $Na_2SO_4$ , filtered and concentrated under pressure. The crude extract was purified by HPLC (90% methanol followed by 100% methanol) to yield PbTx acid naphthalene-2-yl ester **8** (6.4 mg, 55% yield). <sup>1</sup>H NMR ([ $D_6$ ]acetone):  $\delta$  = 7.88 (dd,  $J$  = 8.1, 12.9 Hz, 2 H), 7.91 (d,  $J$  = 8.1 Hz, 1 H), 7.68 (d,  $J$  = 1.84 Hz, 1 H), 7.53 (m, 2 H), 7.34 (dd,  $J$  = 2.14, 9.7 Hz, 1 H), 6.47 (s, 1 H), 5.94 (s, 1 H), 5.75 (dd,  $J$  = 5.4, 10.9 Hz, 1 H), 5.66 (m, 2 H), 4.39 ppm (m, 1 H); <sup>13</sup>C NMR ([ $D_6$ ]acetone):  $\delta$  = 166.45, 163.67, 161.82, 150.04, 139.84, 136.92, 135.01, 132.57, 130.29, 128.89, 128.77, 128.52, 127.62, 127.53, 126.70, 122.48, 119.51, 116.41 ppm; HRMS (ESI): calcd for  $C_{60}H_{77}NO_{15}$ : 1037.5262 [ $M+H$ ]<sup>+</sup>; found: 1037.5283.

**Procedure C: Preparation of the ether analogue 9**—PbTx-3 (30.9 mg, 34.48  $\mu$ mol) was added at 0  $^{\circ}C$  to a solution of NaH (1.65 mg, 68.75  $\mu$ mol) and NaI (6.2 mg, 41.36  $\mu$ mol) in anhydrous THF (10 mL) under argon. The reaction mixture was allowed to stir for 1 h at 0  $^{\circ}C$  before 2-(bromomethyl)naphthalene (11.4 mg, 51.56  $\mu$ mol) dissolved in anhydrous DMF (500  $\mu$ L) was added. The mixture was stirred overnight at room temperature, quenched with a saturated solution of ammonium chloride, and the aqueous layer was extracted with  $Et_2O$  (4  $\times$  10 mL). The organic layers were then combined, washed with water (10 mL), and brine (10 mL), dried over  $Na_2SO_4$  and filtered. The solvent was evaporated under pressure and the crude extract was purified by HPLC (90% methanol followed by 100% methanol) to give analogue **9** (23.2 mg, 65% yield). <sup>1</sup>H NMR ([ $D_6$ ]acetone):  $\delta$  = 7.83 (m, 3 H), 7.69 (s, 1 H), 7.45 (m, 2 H), 7.38 (dd,  $J$  = 1.6, 8.5 Hz, 1 H), 5.77 (dd,  $J$  = 5.5, 11.0 Hz, 1 H), 5.68 (m, 2 H), 5.04 (d,  $J$  = 2.3 Hz, 1 H), 4.84 (s, 1 H), 4.44 ppm (d,  $J$  = 10.5 Hz, 1 H); HRMS (ESI): calcd for  $C_{61}H_{80}O_{14}$ : 1037.5626 [ $M+H$ ]<sup>+</sup>; found: 1037.5657.

## Acknowledgements

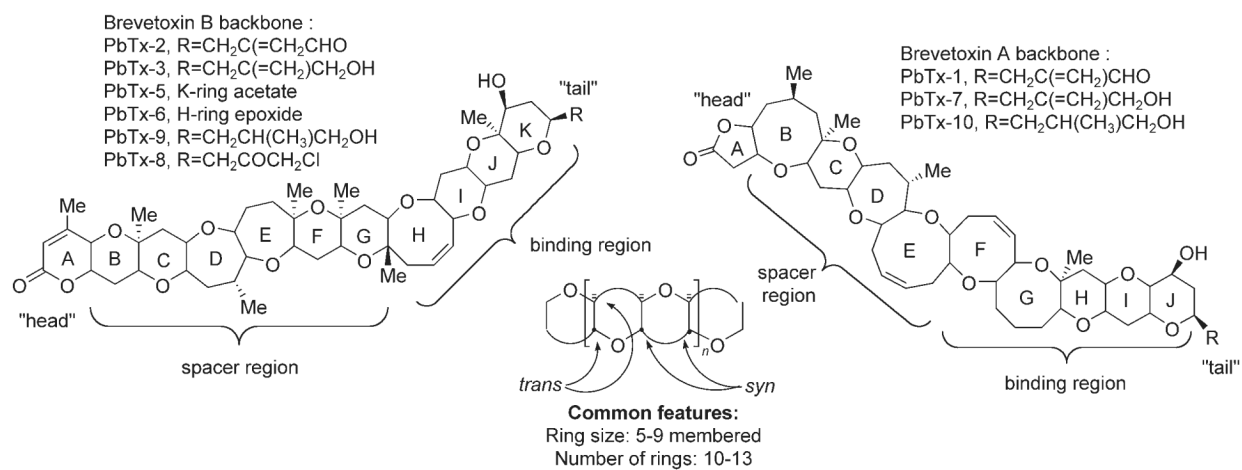
Support for this research was provided by grants from PO1 ES10594 and ES05705, the National Institute of Environmental Health Sciences, (National Institute of Health, the Department of Health and Human Services). We would like to thank Dr. Jon Clardy (Harvard Medical School, Boston, MA) for communicating original structural coordinates of brevetoxins. We would also like to thank Dr. A. Bourdelais, S. Niven, J. Lamberto, and C. Helak for isolation and purification of native toxins. Photograph of the Florida Red Tide is courtesy of Paul Schmidt, Charlotte Sun Herald, FL, Photomicrograph of the dinoflagellate *Karenia brevis* is courtesy of Dr. Carmelo Tomas, Center for Marine Science, UNC Wilmington, NC.

## References

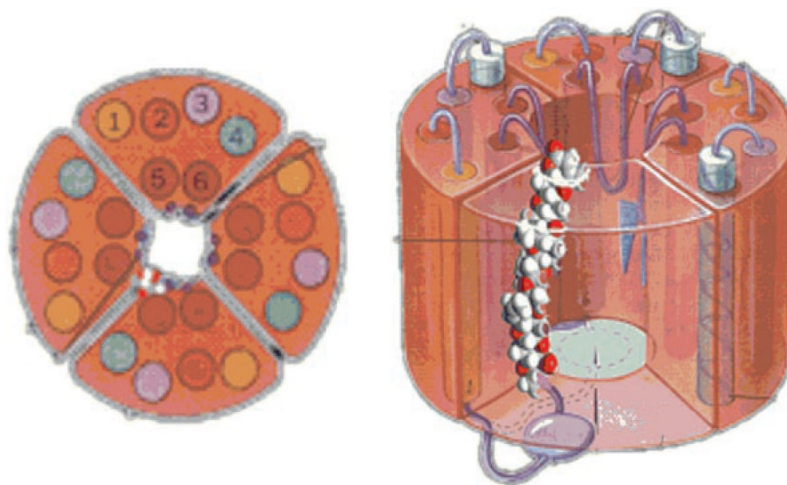
- [1] a). Lin YY, Risk M, Ray SM, Van Engen D, Clardy JC, James JC, Nakanishi K. *J. Am. Chem. Soc.* 1981;103:6773–6775. b) Lee MS, Repeta DJ, Nakanishi K, Zagorski MG. *J. Am. Chem. Soc.* 1986;108:7855–7856. c) Chou HN, Shimizu Y, Van Duyne G, Clardy JC. *Tetrahedron Lett*



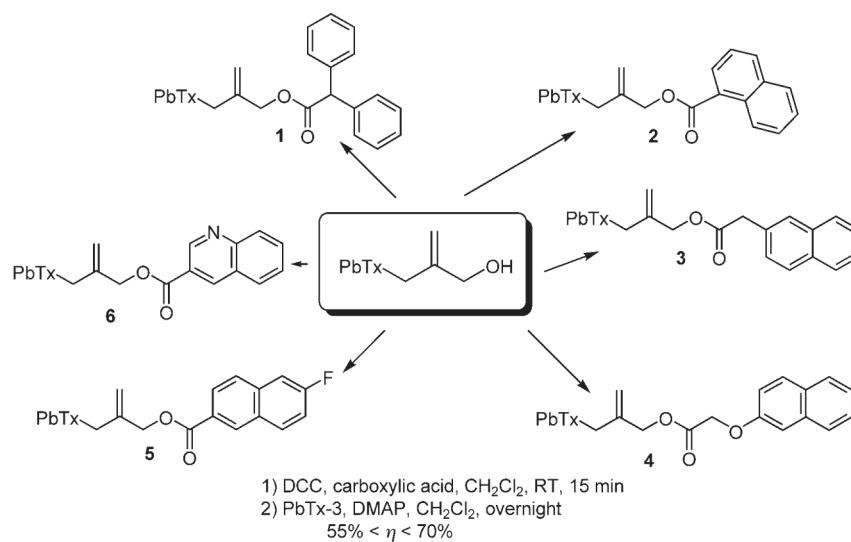
- 1985;26:2865–2868. d) Golik J, James JC, Nakanishi K, Lin YY. *Tetrahedron Lett* 1982;23:2535–2538. e) Shimizu Y, Chou HN, Bando H. *J. Am. Chem. Soc* 1986;108:514–515. f) Pawlak J, Tempesta MS, Golik J, Zagorski MG, Lee MS, Nakanishi K, Iwashita T, Gross ML, Tomer KB. *J. Am. Chem. Soc* 1987;109:1144–1150.
- [2] a). Bossart GD, Baden DG, Ewing RY, Roberts B, Wright SD. *Toxicol. Pathol* 1998;26:276–282. [PubMed: 9547868] b) Trainer VL, Baden DG. *Aquat. Toxicol* 1999;46:139–148. c) Martin DF, Martin BB. *J. Chem. Educ* 1976;53:614–617. [PubMed: 988037]
- [3] a). Sims JKA. *Ann. Emerg. Med* 1987;16:1006–1014. [PubMed: 3307551] b) Baden DG, Flemming LE, Bean JA. *Handbook of Clinical Neurology* 1995;21:141–175.
- [4] a). Pierce RH. *Toxicon* 1986;24:955–965. [PubMed: 3824403] b) Backer LC, Fleming LE, Rowan A, Cheng Y-S, Benson J, Pierce RH, Zaias J, Bean J, Bossart GD, Johnson D, Quimbo R, Baden DG. *Harmful Algae* 2003;2:19–28. [PubMed: 19081765]
- [5] a). Gawley RE, Rein KS, Jeglitsch G, Adams DJ, Theodorakis EA, Tieves J, Nicolaou KC, Baden DG. *Chem. Biol* 1995;2:533–541. [PubMed: 9383457] b) Gawley RE, Rein KS, Kinoshita M, Baden DG. *Toxicon* 1992;30:780–785. [PubMed: 1324537] c) Rein KS, Lynn B, Gawley RE, Baden DG. *J. Org. Chem* 1994;59:2107–2113. d) Rein KS, Baden DG, Gawley RE. *J. Org. Chem* 1994;59:2101–2106. e) Baden DG, Rein KS, Gawley RE, Jeglitsch G, Adams DJ. *Nat. Toxins* 1994;2:212–221. [PubMed: 7952946]
- [6] a). Poli MA, Mende TJ, Baden DG. *Mol. Pharmacol* 1986;30:129–135. [PubMed: 2426567] b) Trainer VL, Thomsen WJ, Catterall WA, Baden DG. *Mol. Pharmacol* 1991;40:988–994. [PubMed: 1661842] c) Rein KS, Baden DG, Gawley RE. *J. Org. Chem* 1994;59:2101–2106.
- [7] a). Jeglitsch GA, Rein KS, Baden DG, Adams DJ. *J. Pharmacol. Exp. Ther* 1998;284:516–524. [PubMed: 9454792] b) Purkerson SL, Baden DG, Fieber LA. *Neurotoxicology* 1999;20:909–920. [PubMed: 10693972] c) Schreibmayer W, Jeglitsch GA. *Biochim. Biophys. Acta Biomembr* 1992;1104:233–242. d) Westerfield M, Moore JW, Kim YS, Padilla GM. *Am. J. Physiol* 1977;232:C23–C29. [PubMed: 556889] e) Wu CH, Huang JMC, Vogel SM, Luke VS, Atchison WD, Narashi T. *Toxicon* 1985;23:481–487. [PubMed: 2411016]
- [8]. Matile D, Berova N, Nakanishi K. *Chem. Biol* 1996;3:379–392. [PubMed: 8807867]
- [9]. Abraham WM, Bourdelais AJ, Sabater JR, Ahmed A, Lee TA, Serebriakov I, Baden DG. *Am. J. Respir. Crit. Care Med* 2005;171:26–34. [PubMed: 15447946]
- [10]. Purkerson-Parker SL, Fieber LA, Rein KS, Podona T, Baden DG. *Chem. Biol* 2000;7:385–393. [PubMed: 10873835]
- [11]. Abraham WM, Sielczak MW, Ahmed A, Cortes A, Laredo IT, Kim J, Pepinsky B, Benjamin CD, Leone DR, Lobb RR. *J. Clin. Invest* 1994;93:776–787. [PubMed: 8113411]
- [12]. Abraham WM, Gill A, Ahmed A, Sielczak MW, Laredo IT, Botvinnikova Y, Lin KC, Pepinsky B, Leone DR, Lobb RR. *Am. J. Respir. Crit. Care Med* 2000;162:603–611. [PubMed: 10934094]
- [13]. Abraham WM, Ahmed A, Serebriakov I, Carmillo AN, Ferrant J, de Fougere AR, Garber EA, Gotwals PJ, Koteliensky VE, Taylor F. *Am. J. Respir. Crit. Care Med* 2004;164:97–104. [PubMed: 14578216]
- [14]. Dodd PR, Hardy JA, Oakley AE, Edwardson JA, Perry EK, Delaunoy J-P. *Brain Res* 1981;226:107–118. [PubMed: 7296283]



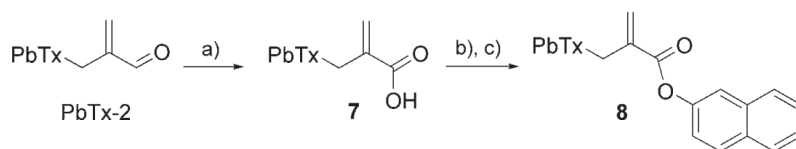
**Scheme 1.**  
 Natural brevetoxins.



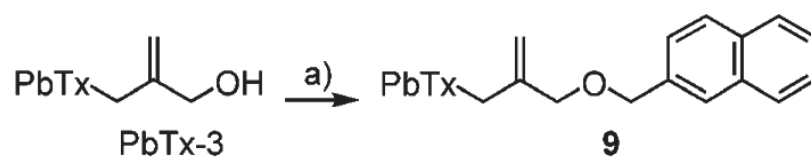
**Figure 1.**  
Brevetoxins receptor site.

**Scheme 2.**

Synthesis of  $\beta$ -naphthoyl-PbTx analogues. a) DCC, carboxylic acid,  $\text{CH}_2\text{Cl}_2$ , RT, 15 min; b) PbTx-3, DMAP,  $\text{CH}_2\text{Cl}_2$ , overnight  $55\% < \eta < 70\%$ .

**Scheme 3.**

Synthesis of PbTx acid naphthalene-2-yl ester. a) NaClO<sub>2</sub>, Na<sub>2</sub>HPO<sub>4</sub>, 2-methylbut-2-ene, *t*BuOH, RT, 4 h, 85%; b) DCC, CH<sub>2</sub>Cl<sub>2</sub>, RT, 15 min; c) 2-naphthol, DMAP, CH<sub>2</sub>Cl<sub>2</sub>, overnight, 55%.

**Scheme 4.**

Synthesis of an ether analogue of  $\beta$ -naphthoyl-Pbtx. a) NaH, NaI, THF, 0 °C, 1 h; b) 2-(bromomethyl)naphthalene, DMF, 0 °C to RT, overnight, 65%.

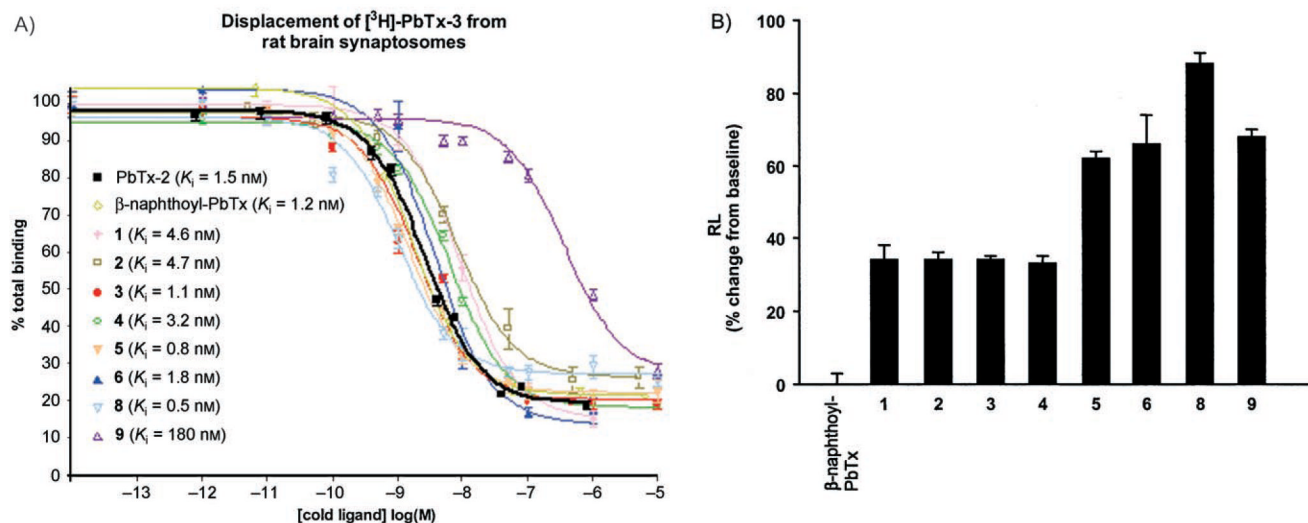


**Figure 2.**

A) Inhibition of binding of [<sup>3</sup>H]-PbTx-3 to site 5 of the voltage-gated sodium channel by the β-naphthoyl-PbTx analogues. Points represent the mean of triplicate determinations. Error bars represent one standard error of the mean. B) Bronchoconstrictor effects measured as the percentage increase in lung resistance from baseline. Analysis of 5–10 breaths is used for each determination of RL.

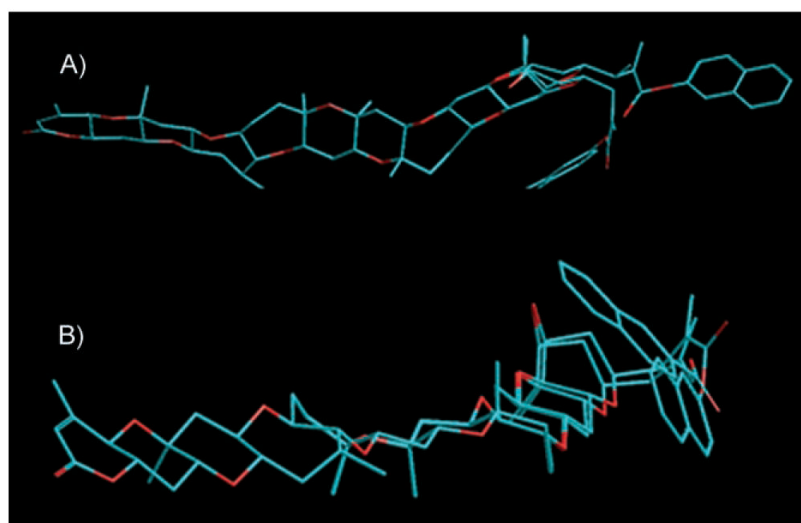


**Figure 3.**  $\beta$ -naphthoyl-PbTx and “reverse  $\beta$ -naphthoyl-PbTx” **8** in MM +-minimized conformations. A) is an overlay of the “reverse  $\beta$ -naphthoyl-PbTx” **8** and  $\beta$ -naphthoyl-PbTx derivatives in the folded form showing the extend of naphthyl overlap. B) is an overlay of the minimum energy conformers of the folded and unfolded form of the “reverse ester” **8**.



**Table 1**

Summary of equilibrium dissociation constants and RL percentage increases.

Compound	$K_i$ [nM] <sup>[a]</sup>	S.E. <sup>[b]</sup>	RL <sup>[c]</sup>	S.E. <sup>[b]</sup>
PbTx-2	1.5	0.41	226	21
$\beta$ -naphthoyl-PbTx	1.2	0.04	0	3
<b>1</b>	4.6	0.85	34	4
<b>2</b>	4.7	0.16	34	2
<b>3</b>	1.1	0.20	34	1
<b>4</b>	3.2	0.32	33	2
<b>5</b>	0.8	0.05	62	2
<b>6</b>	1.8	0.76	66	8
<b>8</b>	0.5	0.05	88	7
<b>9</b>	180	0.38	68	2

<sup>[a]</sup>Total binding was measured using the described centrifugation technique.[6a] Competitor concentration ranged from 0 to 10  $\mu$ M and the concentration of [<sup>3</sup>H]-PbTx-3 was held at 1.5 nM. Nonlinear regression analysis was performed using GraphPad prism. All derived values are the mean of at least three experiments, with duplicate or triplicate determination at each concentration of inhibitor in each experiment.

<sup>[b]</sup>Standard error of the mean.

<sup>[c]</sup>Percentage increase from baseline. To measure RL, the proximal end of the endotracheal tube is connected to a pneumotrachograph, and the signals representing flow and transpulmonary pressure are recorded by computer. Respiratory volume is obtained by digital integration of the flow signal so that RL is calculated from transpulmonary pressure and flow at isovolumetric points. Analysis of 5–10 breaths is used for each determination of RL.  $\beta$ -naphthoyl-brevetoxin analogues were delivered into the airways as aerosols.